Materials Science-Poland, 30(3), 2012, pp. 204-211
http://www.materialsscience.pwr.wroc.pl/
DOI: 10.2478/s13536-012-0026-z

Dry sliding wear behaviour of fly ash particles reinforced AA 2024 composites

J. BABU RAO*[1], D. VENKATA RAO[1], K. SIVA PRASAD[2], N. R. M. R. BHARGAVA[1]

[1]Dept. of Metallurgical Engineering, Andhra University, Visakhapatnam - 530 003, India

[2]Advanced Materials Processing Lab, Dept. of Metallurgical and Materials Engineering, National Institute of Technology- Trichy- 620 015, India

AA 2024 alloy has been melted and cast in a permanent cast iron mould in the form of 18 mm Φ fingers. The synthesis of AA2024 alloy – 5wt.% fly ash composite was made by stir cast technique. A uniform distribution of fly ash particles in the matrix phase was obtained. Good bonding between the matrix and reinforcement was also achieved. Dry sliding wear behavior of the alloy and the composite has been investigated using a pin-on-disc wear tester. The investigation was carried out at a fixed sliding velocity of 2.0 m/s, track diameter of 60 mm and load ranging from 0.5 kgf to 1.5 kgf (4.9 – 14.7 N). SEM studies were carried out to assess the wear behavior of the alloy and the composite. The composite showed better wear resistance than the base alloy for the lower loads. However, for the higher loads and longer sliding distances, the wear in the composite was extensive due to the existence of fractured and dislodged fly ash particles in the alloy matrix.

Keywords: *metal-matrix composite, Al-fly ash composites, wear testing, sliding wear, electron microscopy.*

1. Introduction

The expeditious advancement of technology in the past decades has resulted in the need for new multifunctional materials which possess characteristics not obtainable from any individual material. Metal matrix composites (MMCs) are advanced materials obtained by a combination of two or more materials in which tailored properties can be realized. The composites possess significantly higher strength and stiffness than unreinforced materials. Many of the applications for which MMCs are desirable also require enhanced tribological performance. Aluminum is a potentially important material for tribological applications because of its low density and high thermal conductivity. However, aluminum itself exhibits poor tribological properties. Therefore, the study of the tribological behaviour of aluminum based materials is becoming increasingly important. Aluminum metal matrix composites (AMMCs) possess much higher specific strength and stiffness, higher wear resistance and lower thermal expansion coefficient in comparison to their base alloy matrices due to the incorporation of suitable particles or fibers into the metal matrix [1, 2].

Considerable amounts of research on the dry sliding wear behaviour of aluminum metal matrix composites (AMMCs) have been carried out. The comprehensive reviews of this research were done by P. K. Rohatgi, A.P. Sannino, R.L. Deuis [3–5]. The reinforcements typically used in AMMCs are SiC and Al_2O_3 particles, whiskers and short fibers. However, for many applications these composites are too expensive to permit their widespread use. There has been an increasing interest in the composites containing low density and low cost reinforcements [6–9]. P. K. Rohatgi et. al. [10] studied the tribological performance of A206 aluminum alloy containing silica sand particles. The test results show that the addition of silica sand particles decreases the friction coefficient of Mg modified A206 alloy, but the wear rate of the composites increases with the increase in the applied pressure and

*E-mail: baburaojinugu@yahoo.com

silica sand content. Dry sliding wear behaviour of silicon particles-reinforced aluminum matrix composites was reported by Sun Zhiqiang et. al. [11]. In their work, a ring on rock wear testing machine was used to study the wear properties of powder metallurgy aluminum matrix composites 9Si/Al-Cu-Mg. The results show that silicon particle-reinforced composites exhibit reduced wear loss as compared with the unreinforced alloy specimens. Quartz (SiO_2p) reinforced chilled metal matrix composites for automotive applications were developed by Joel Hemanth [12]. In his study, he observed that the wear rate of the chilled composite increased as the applied load was increased. This increase was lower than that of the Al-12% Si alloy matrix. It was also observed that the wear resistance of the chilled composite had increased along with the increasing the dispersoid content.

Among the various low cost and low density reinforcements used, fly ash is one of the cheapest, low density reinforcements available in large quantities as solid waste by-product from combustion of coal in thermal power plants. There are two types of fly ash particles namely cenosphere particles with density below 1.0 g/cm^3, and precipitator particles with density between 2.0 – 2.5 g/cm^3. Fly ash is generally composed of crystalline compounds such as quartz, mullite, hematite; glassy compounds like silica glass, and other oxides [13, 14]. Hence, the composite in which fly ash is used as reinforcement can overcome the cost barrier for widespread applications in automotive and small engine industry. It is therefore expected that the incorporation of fly ash particles in aluminum alloy will promote yet another use of this low-cost and waste by-product thereby, reducing the cost of aluminum products.

M Ramachandra et. al. [15, 16] showed that increasing the fly ash content in Al-Si alloy matrix increases the wear resistance and reduces the friction coefficient. His MMCs exhibited better wear resistance (20 – 30 % improvement) than Al-Si alloy, due to their superior load bearing capacity. Sudrashan et. al. [17] reported that the dry sliding wear of fly ash particles reinforced A356 Al-composites. Dry sliding wear behaviour of aluminum syntactic foam was discussed by D. P. Mondal et. al. [18].

The alloys most commonly used in aluminum matrix composites are Al-Si and Al-Cu based alloys. In addition, Al-Mg and Al-Zn based alloys have also been investigated as potential matrix materials for AMMCs. AA 2024 alloy, because of its high tensile and yield strength, is the most widely used aluminum-copper alloy for manufacturing forgings as well as rivets in automotive and aircraft industry. The literature available on AA 2024 alloy – fly ash composites is limited. Very little information is available about the influence of fly ash particles on ALFA composites in the tribological data. Therefore the present investigation makes an attempt to synthesize the AA 2024 alloy – fly ash composites by stir casting route and tries to study the dry sliding wear behaviour of these composites.

2. Materials and methods

2.1. Synthesis of Al – 5wt.% fly ash composite

The matrix material used in this study was Al-Cu-Mg alloy (AA2024). Its chemical composition is shown in Table 1. The reinforcement material used in this study was procured from Thermal Power Plant of Rashtriya Ispath Nigam Limited, Visakhapatnam Steel Plant, Visakhapatnam, India. The chemical composition of the fly ash in as-received-condition is given in Table 2. The fly ash sample of 500 grams was put into a graphite crucible and allowed to preheat in a muffle furnace at 800 °C for 3 hours to test the loss on ignition. Consequently, it was found to amount to 2.4 %. After cooling to room temperature, the preheated fly ash was washed in distilled water and the carbon which had creamed up was removed. Then the sample was dried up at 110 °C for 48 hours to get rid of water. The dried fly ash was sieved for 15 minutes with a Rotap sieve shaker, using BSS meshes ranging in size from 100 to 350. It was found that more than 70 wt.% of the sample retained in -200 +350 BSS meshes. The

Table 1. Chemical composition of AA 2024 alloy, wt.%.

Cu	Mg	Si	Fe	Mn	Ni	Pb	Sn	Zn	Ti	Al
4.52	1.938	0.066	0.663	0.131	0.075	0.029	0.021	0.118	0.013	Balance

Table 2. Chemical composition of as received fly ash, wt.%.

SiO_2	Al_2O_3	Fe_2O_3	TiO_2	CaO	MgO	Na_2O	K_2O
58.41	30.40	8.44	2.75	1.3	1.53	1.0	1.98

Table 3. Properties of as received fly ash.

Particle size	60 µm
Total evaporable moisture content	1.54 %
Loss on ignition	2.4 %

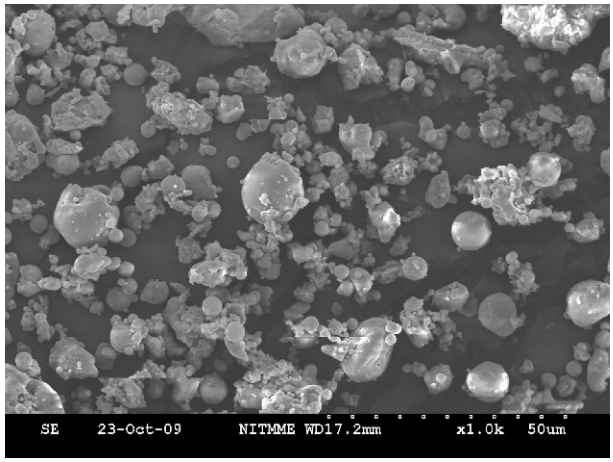

(a)

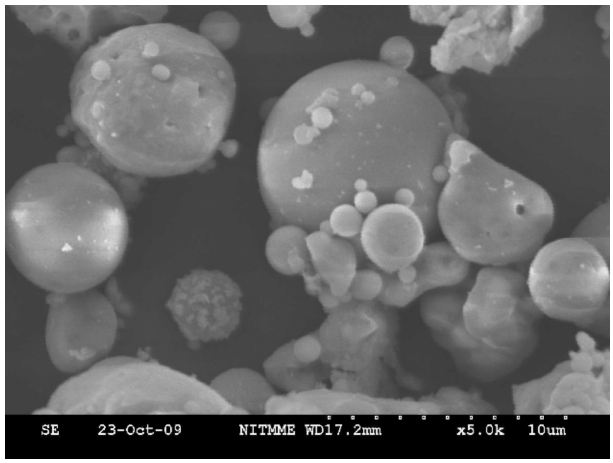

(b)

Fig. 1. SEM micrograph of as- received fly ash particles used in fabricating the composite. (a) at lower and (b) at higher magnification.

average size of the fly ash particles was equal to 60 microns; hence this size was chosen as the reinforcement for synthesis of the Al. – 5wt.% fly ash composite.

Figs. 1a and b show the scanning electron micrographs of the fresh fly ash after heat treatment. From this figure it is evident that the majority of the fly ash particles are spherical in nature and are of precipitator type. The morphology of the fly ash particles is controlled by combustion temperature and cooling rate at the thermal power plant. The X-ray diffraction (XRD) pattern of fly ash in the as-received-condition is shown in Fig. 2, which depicts the phases that are present in the fly ash. They are mainly silica (SiO_2), alumina (Al_2O_3) and mullite ($3Al_2O_3$. $2SiO_2$).

The synthesis of the Al-fly ash composite was carried out by stir casting route. The cylindrical fingers (18 mm Φ and 170 mm length) of AA 2024 alloy were placed in a graphite crucible and melted in an electric furnace. After maintaining the temperature between 770 and 800 °C, a vortex was created using a mechanical stirrer. While stirring was in progress, the preheated fly ash particulates, which were kept at 800 °C for 2 h, were introduced into the melt. The molten metal was stirred at 400 rpm under argon gas atmosphere. The stirring was continued for about 5 minutes after addition of fly ash particles to achieve its uniform distribution in the melt. While stirring, small pieces of magnesium (0.5wt.%) were added to the molten metal to enhance the wettability of the fly ash particles with the melt. The melt with reinforcement was in stirring condition; it was cast into a preheated (200 °C) S.G. iron mould of 18 mm diameter and 170 mm length. The homogenization treatment was carried out at 200 °C for 24 h.

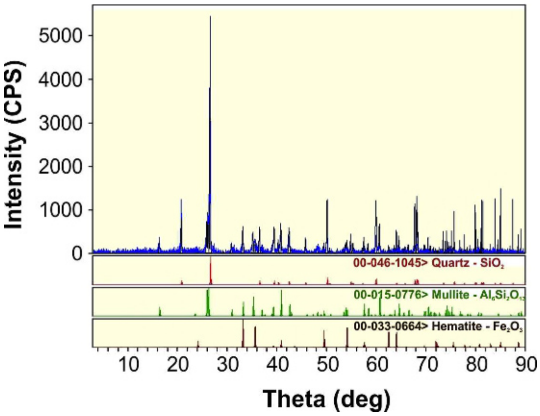

Fig. 2. X-ray diffractogram of as- received fly ash.

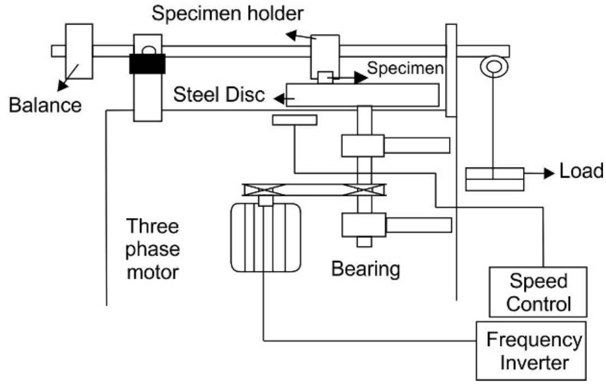

Fig. 3. Pin-on-disc wear tester (Model: Ducom TR-20 LE).

Scanning electron microscope (Model: SEM – Quanta 400, FEI -Netherlands) with EDAX energy dispersive X-ray spectroscopy (EDS) was used to evaluate the morphological changes and perform the elemental analysis of certain phases observed in the fly ash particles. Further SEM studies were carried out on the composite before and after wear tests. The hardness of the alloy and composite was evaluated using Leco Vickers hardness tester (Model: LV 700- USA). An average of ten readings was taken for each hardness value.

2.2. Wear tests

Dry sliding wear tests have been carried out on a pin- on- disc apparatus (Model: Ducom TR-20 LE) by sliding a cylindrical pin against the surface of hardened steel disc (with a hardness value of HRC 62) under ambient condition, as shown in Fig. 3. The disc was ground to a smooth surface finish and renewed for each test. The wear test specimens were prepared from the alloy and composite castings in the dimensions of 10 mm Φ and 30 mm length. Prior to testing, the test samples were polished with emery paper and cleaned in acetone, dried and then weighed using an electronic balance (Model: Sartorius Research R 200 D-Germany) with a resolution of 0.1 mg. The samples were placed on the wear disc and the sliding wear tests were carried out at various loads, time and sliding distance. The test was conducted in a load range of 0.5 – 1.5 kgf (4.9 – 14.7 N) at a sliding velocity of 2.0 m/s and at sliding distance of 1.2 – 2.4 km. After each test, the specimens were removed, cleaned in acetone and weighed with an electronic balance within an accuracy of 0.1 mg. For each load, the volume loss from the surface of each specimen was determined as a function of sliding distance and applied load. The wear rate (K) was defined as the volume loss (V), divided by the sliding distance (L). Hence, the volumetric wear rate (K) was calculated from the weight loss measurement and expressed in terms of mm^3/km. The friction force (F) was continuously monitored during the wear test for determining the coefficient of friction (μ).

3. Results and discussion

Figs. 4a and 4b show the typical optical microstructures of the AA 2024 alloy and AA 2024 alloy – 5wt.% fly ash composite, respectively. The alloy specimens are hypoeutectic alloys consisting of a soft aluminum solid solution matrix (α) and a hard $CuMgAl_2$ phase. The microstructure is composed of white (α) primary grains and a dark eutectic (α + $CuMgAl_2$). The microstructure of the Al-fly ash composite reveals that there is a uniform distribution of fly ash particles in the base matrix of Al-2024 alloy. Fig. 4c illustrates the typical scanning electron micrograph of AA 2024 alloy – 5wt.% fly ash composite; from this figure it is clearly seen that there are no voids and discontinuities in the composite and that there is a good interfacial bonding between the fly ash particles and the matrix.

The hardness values of the AA 2024 alloy and AA 2024 alloy – 5% fly ash (ALFA) composite were 84 and 124 VHN respectively. The presence of fly ash results in hardness increase of the alloy from 84 VHN to 124 VHN. This increase is due to the fact that the fly ash particles consist of alumina and silica, which are hard in nature.

Figs. 5a, 5b and 5c show the wear rate as a function of sliding distance for 0.5, 1.0 and 1.5 kgf (4.9, 9.8, and 14.7 N) applied loads. It can be seen that the wear rate of the alloy decreases with the increase in sliding distance from 1.2 km to 1.8 km and then a slight increase in the wear rate is observed for all the applied loads. The wear processes in materials are similar to the plastic deformation phenomenon which leads to cold working of the material. Hence, the decrease in wear rate of the material under investigation is due to the strain hardening behaviour of soft α -matrix in the presence of hard $CuAl_2$ (θ) phase in the matrix. While AA 2024 – 5wt.% composite shows lower wear rates at the low loads (0.5 and 1.0 kgf (4.9 and 9.8 N)) due to the presence of hard fly ash particles in the alloy matrix, at the higher loads and longer sliding distances the wear rate increases more for the composite than for the alloy, as shown in Fig. 6. This might be due to the delamination and chipping out of the fly ash particles from the matrix.

Figs. 7 and 8 show the morphology of the wear scar of AA 2024 alloy and AA 2024 alloy- fly ash (5wt.%) composite. The presented morphology was obtained at wear loads of 0.5 kgf and 1.5 kgf for a sliding distance of 2.4 km, at a sliding velocity of 2.0 m/s. At a load of 0.5 kgf for a track distance of 2.4 km, the AA 2024 alloy exhibits rough worn surface (Fig. 7a), while the surface of the AA 2024 – 5wt.% fly ash composite is relatively less rough (Fig. 7b). It is observed that as the applied load increases from 0.5 kgf to 1.5 kgf, the wear tracks on the worn surfaces of AA 2024 alloy and AA 2024 – 5wt.% fly ash composite change gradually from scratches to deep grooves as shown in Figs. 8a and 8b. While the worn surfaces of the alloy show

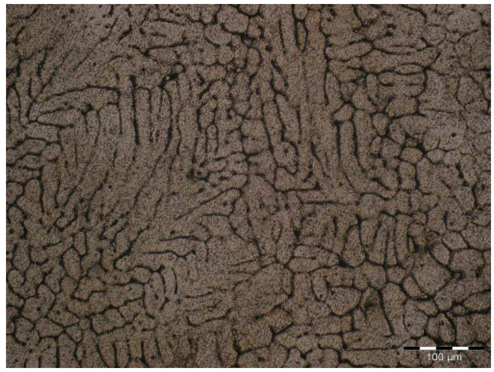

(a)

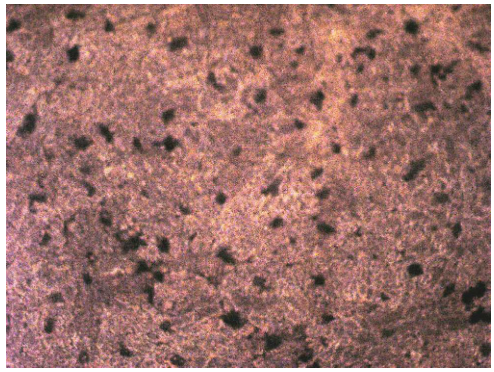

(b)

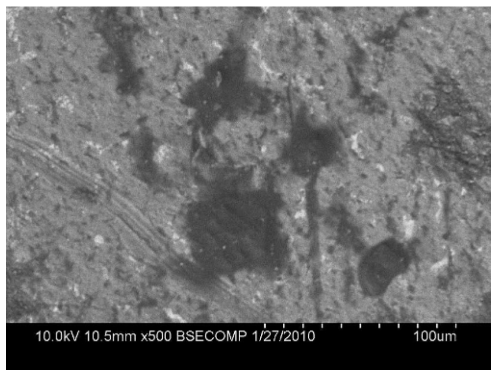

(c)

Fig. 4. (a and b) Optical photographs of the microstructure of as cast AA 2024 alloy and AA 2024 – 5wt.% fly ash composite, at 100× magnification, Etchant: Keller's reagent. (composition: HF = 1.0 cm^3, HCL = 1.5 cm^3, HNO_3 = 2.5 cm^3 and H_2O = 95 cm^3). (c) SEM image of AA 2024 alloy – 5wt.% fly ash composite showing the interface between fly ash particles and the matrix.

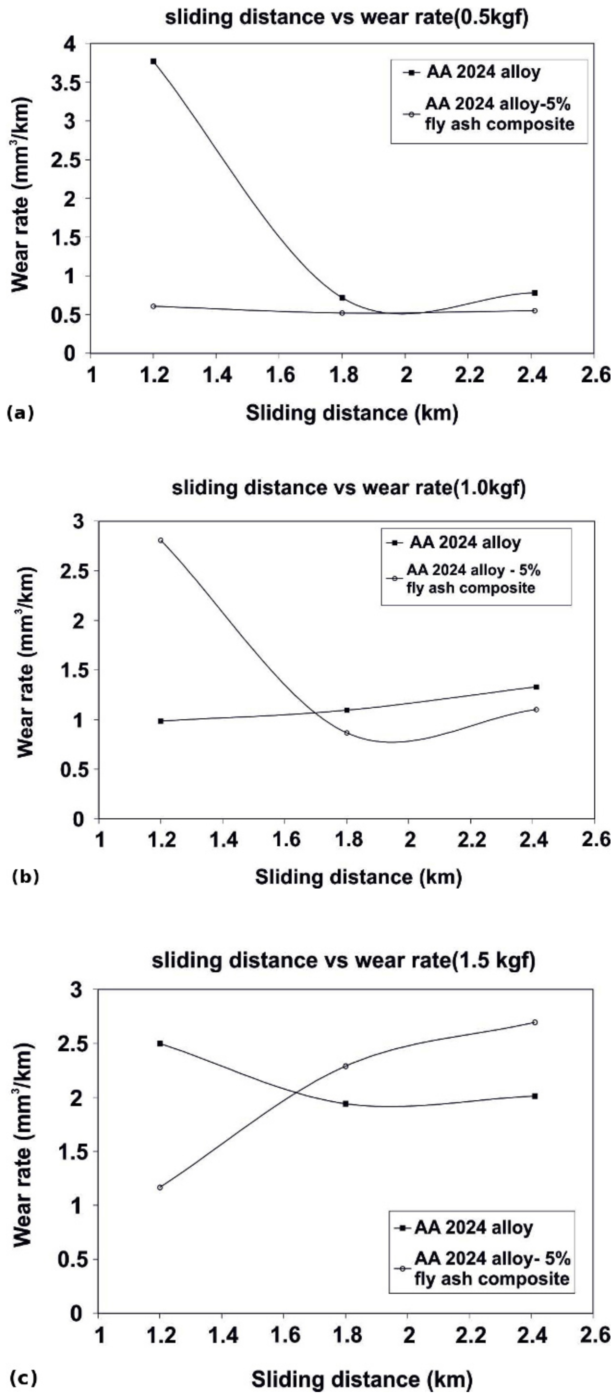

Fig. 5. (a) Variation of wear rate as a function of sliding distance at 0.5 kgf applied load; (b) Variation of wear rate as a function of sliding distance at 1.0 kgf applied load; (c) Variation of wear rate as a function of sliding distance at 1.5 kgf applied load.

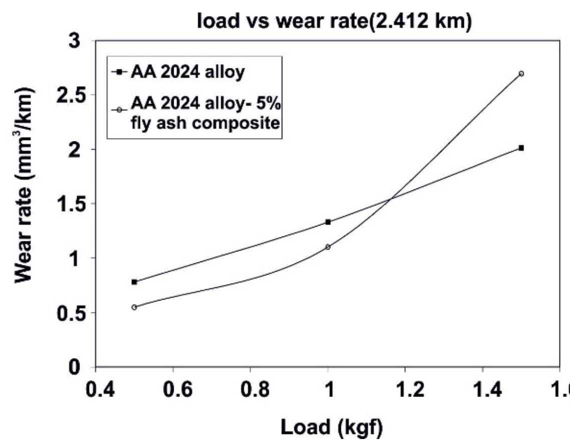

Fig. 6. Variation of wear rate as a function of different applied loads at sliding distance of 2.4 km

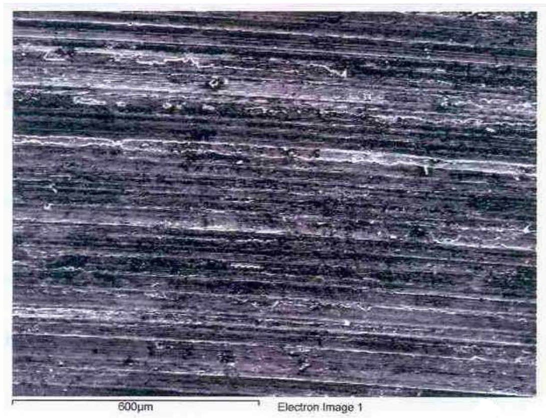

(a)

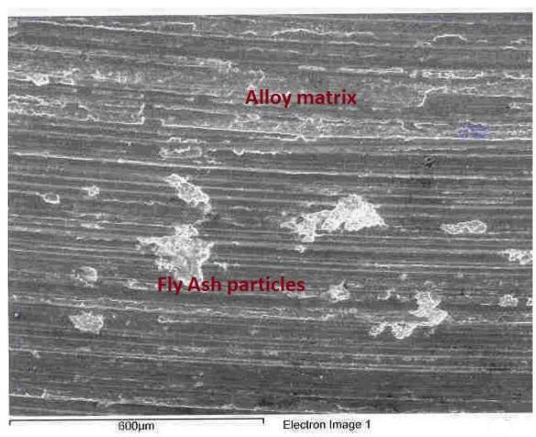

(b)

Fig. 7. (a) Worn surface of AA 2024 alloy at 0.5 kgf, 2.4 km; (b) Worn surface of AA 2024 alloy – 5wt.% fly ash composite at 0.5 kgf, 2.4 km.

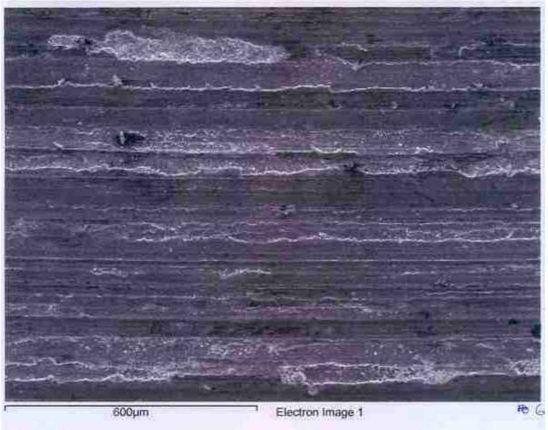

(a)

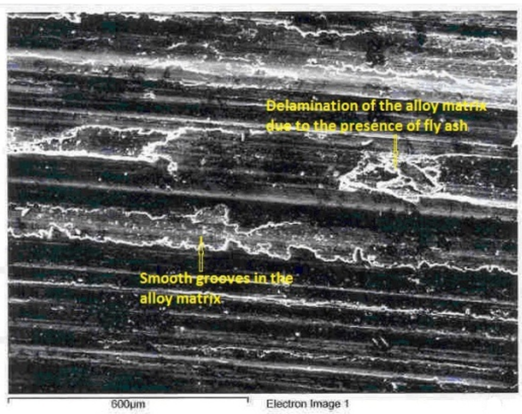

(b)

Fig. 8. (a) Worn surface of AA 2024 alloy at 1.5 kgf, 2.4 km; (b) Worn surface of AA 2024 alloy – 5wt.% fly ash composite at 1.5 kgf, 2.4 km.

deeper and wider scratches, the composite exhibits smooth surface with the ploughing strips which are very shallow. It is observed that the wear increases as the load increases for both the alloy and the composite. Hence, the wear behavior of the AA 2024 alloy and AA 2024 – 5wt.% fly ash composite strongly depends on the applied load; the wear increases proportionally along with the increase of the applied loads. The reasons for the poor wear behavior of the alloy and the composite at higher loads might be due to the occurrence of abrasion, delamination and chipping out of the reinforcement particles from the matrix.

Number of grooves, mostly parallel to the sliding direction, is evident on all the worn pins. Grooving and scratching appear more severe at the higher loads of 1.5 kgf. Such features are characteristic of abrasion, in which hard asperities of steel counterface or hard reinforced particles, which lie between the contacting surfaces, plough or cut into the pin, causing wear by removing small fragments of material. The abrasion takes place primarily via ploughing, in which material is displaced on either side of the abrasion groove without being removed, or through wedge forming, where tiny wedge shaped fragments are worn only during the initial contact with an abrasive particle [19]. The abrasion is extensive in the tested Al-fly ash composite due to the presence of dislodged and fractured fly ash that gets trapped in the sliding interface and gets embedded in the counterface, contributing to abrasive wear. In addition, the fractured fly ash particles trapped between the sliding surfaces will also cause abrasion of the steel disc as shown in Figs. 7 and 8.

Delamination is a fatigue-related wear mechanism in which repeated sliding induces sub-surface cracks that gradually grow and eventually shear the surface, forming long and thin wear sheets [20]. Delamination is observed to be more extensive under the higher loads. Delamination involves sub-surface deformation, crack nucleation and crack propagation; increase in load and speed hastens these processes and produces greater wear. The pivotal role of crack formation and growth in delamination also accounts for the higher wear of the composites, as the fly ash-matrix interfaces provide additional void nucleation sites, as well as preferential crack propagation paths. In the present tests, the wear rates for the composite are higher under the sliding distance of 2.4 km and a load of 1.5 kgf, where delamination is significant. This is shown in Fig. 8b.

4. Conclusions

1. Aluminium - fly ash composites were successfully produced by stir casting route.
2. There was a uniform distribution of fly ash particles in the matrix phase and a good

bonding between the matrix and fly ash reinforcements was achieved.

3. The hardness of the composites increased to the value higher than that of the base alloy due to addition of fly ash.
4. The composite showed better wear resistance than the base alloy for the lower applied loads.
5. The wear was extensive in Al-fly ash composite for higher loads and longer sliding distances, due to the presence of dislodged and fractured fly ash particles in the alloy matrix.

Acknowledgements

The authors would like to thank the University Grants Commission, New Delhi, India for their financial support to the work under UGC-MRP (File No: 34 -396/2008 (SR)) scheme; the Department of Metallurgical Engineering, Andhra University College of Engineering, Visakhapatnam, A.P., India for providing necessary support in conducting the experiments. Special thanks to RINL, Visakhapatnam Steel Plant, Visakhapatnam for the supply of fly ash for this study.

References

[1] ROHATGI P.K., In: Invited silver anniversary lecture by American Foundry Society, *AFS Transactions*, 01-133 (2001), 633.
[2] ROHATGI P.K., GUPTA N., DAOUD A., ASM handbook; Casting: vol. 15; *ASM International*; 2008, p.1149-1164.
[3] ROHATGI P.K., LIU Y., RAY S., ASM handbook. Friction, lubrication, and wear technology, vol. 18. *ASM International*; 1992 p.801-811.
[4] SANNINO A.P., RACK H.J., *Wear*, 189 (1995), 1.
[5] DEUIS R.L., SUBRAMANINA C., YELLUP J.M., *Compos Sci Technol*., 57 (1997), 415.
[6] SEAH K.H.W., HEMANTH J., SHARMA S.C., *Materials and Design,* 24(2) (2003), 87.
[7] SIDDIQUEA R., NOUMOWEB A., *Conservation and Recycling*, 53 (2008), 27.
[8] BELGER M.A., ROHATGI P.K., GUPTA N., *TMS annual meeting, (*2006), p. 95-204.
[9] SULAIMAN S., SAYUTI M., SAMIN R., *J. of Materials Processing Technology*, 201 (2008), 731.
[10] ROHATGI P.K., SCHULTZ B.F., DAOUD A., ZHANG W.W., *Tribology International*, 43 (2010), 455.
[11] SUN ZHIQIANG, DI ZHANG, LI GUOBIN, *Materials and Design,* 26 (2005), 454.
[12] HEMANTH J., *Materials and Design,* 30 (2009), 323.
[13] KUMAR V., ABRAHAM ZACHARIA K., SHARMA P., Fly Ash Utilization: Indian Scenario & Case Studies. `http://www.tifac.org.in/news/flyindia.htm` as on 15 April 2007.
[14] MATSUNAGA T., KIM J.K., HARDCASTLE S., ROHATGI P.K., *Materials Science and Engineering- A,* 325 (2002), 333.
[15] RAMACHANDRA M., RADHAKRISHNA K., *Wear,* 262 (2007), 1450.
[16] RAMACHANDRA M., RADHAKRISHNA K., *Journal of Materials Science*, 40 (2005), 5989.
[17] SUDRASHAN, SURAPPA M.K., *Wear,* 256 (2008), 349.
[18] MONDAL D.P., DAS S., NIDHI JHA., 30 (2009), 2563.
[19] QUINN T.J.F., *J. Appl. Phys*., 13 (1962), 33.
[20] ZHANG J., ALPAS A. T., *Acta. Mater*, 45 (1997), 513.

Received 2011-05-09
Accepted 2012-06-28